

Thermal stability and degradation of biological terpolyesters over a broad temperature range

Nuttapol Tanadchangsang,^{1,2} Jian Yu¹

¹Hawai'i Natural Energy Institute, University of Hawai'i at Manoa, Honolulu, Hawaii 96822, USA

²College of Oriental Medicine, Rangsit University, Pathumthani 12000, Thailand

Correspondence to: J. Yu (E-mail: jianyu@hawaii.edu) and N. Tanadchangsang (E-mail: nuttapol.t@rsu.ac.th)

ABSTRACT: Because of high susceptibility to thermal degradation during conventional melt processing of poly(3-hydroxybutyrate) (P3HB) homopolymer, incorporation of a second or third monomer unit in the polyester backbones is expected to reduce the melting temperature and crystallinity, resulting in a controlled thermal degradation with improved stability. In this work, random poly(3-hydroxybutyrate-co-3-hydroxyvalerate-co-4-hydroxyvalerate) (P3HB3HV4HV) terpolyesters biologically synthesized by *Cupriavidus necator* were investigated for the thermal stability and degradation over a broad temperature range (100–300°C) in comparison with P3HB homopolymer. The work revealed that below the complete melting point (around 150°C), the terpolyester exhibited a high thermal stability and became an amorphous semisolid suitable for conventional thermal processing. Size exclusion chromatography plus nuclear magnetic resonance analysis was used to examine the thermal degradation products and the vulnerability of different monomer units at high temperatures (240–290°C). We found that 3HV unit in P3HB3HV4HV copolymers was more vulnerable to thermal degradation than 3HB unit under air. © 2014 Wiley Periodicals, Inc. *J. Appl. Polym. Sci.* **2015**, *132*, 41715.

KEYWORDS: biopolymers and renewable polymers; structure–property relations; thermal properties; properties and characterization

Received 10 June 2014; accepted 25 October 2014

DOI: 10.1002/app.41715

INTRODUCTION

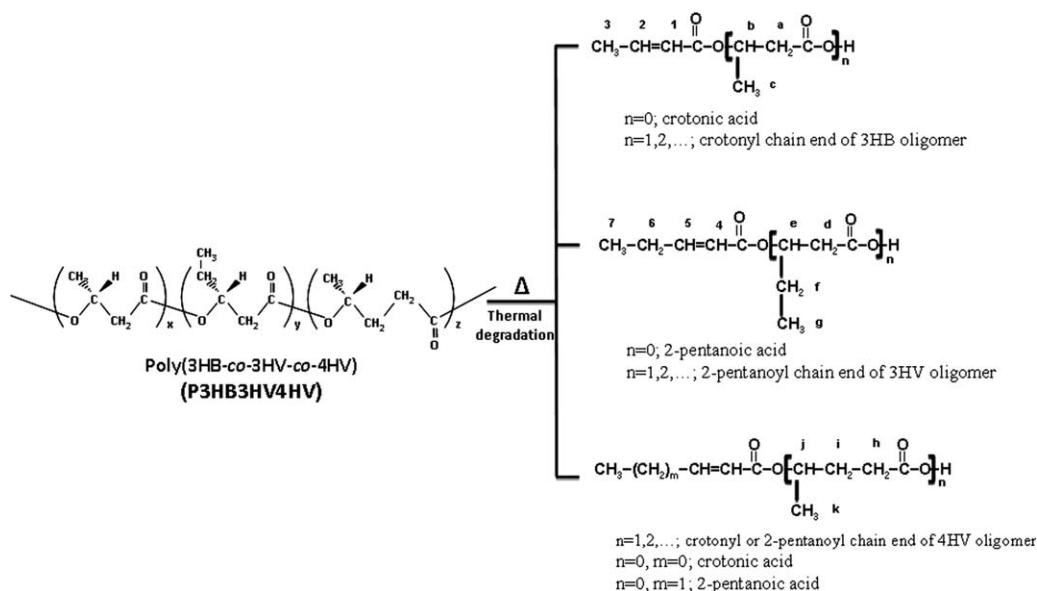
Polyhydroxyalkanoates (PHAs) are biological polyesters synthesized by many microbial species as intracellular carbon and energy reserve.^{1–3} The biopolyesters can be melted and molded like conventional petroleum-based plastics and, after use, completely degraded into benign products via microbial activities.^{4–7} The thermal properties of PHAs are of great interest to polymer processors. Many studies have been conducted on thermal degradation of poly(3-hydroxybutyrate) (P3HB), the most ubiquitous member of PHAs.^{8–17} It has been found that P3HB is highly susceptible to thermal degradation. Because of its high melting point (170–180°C), P3HB is processed around 190°C, above which thermal breakdown of the polyester backbone rapidly occurs, resulting in a significant decrease in molecular weight and, consequently, deterioration of the mechanical properties.⁵ One possible solution is to reduce the melting temperature of bioplastic by introducing a second or even third monomer unit in the PHB backbones such as 3-hydroxyvalerate (3HV) and 4-hydroxyvalerate (4HV). Because of the reduced crystallinity, the melting temperature of copolyesters can be reduced by 40–60°C, depending on the mole percentage of 3HV and 4HV.¹⁸ In this low temperature range (120–150°C), it

is expected that the thermal degradation of poly(3HB-co-3HV-co-4HV) (P3HB3HV4HV) copolymers is under control with improved thermal stability. The PHA bioplastics can therefore be processed like conventional thermoplastics. There is little evidence, however, that a random P3HB3HV4HV or its blends can be processed at a low temperature with improved thermal stability.

The thermal degradation of P3HB proceeds mainly via a random chain scission (*cis*-elimination) reaction, forming a six-member ring structure of 3HB monomer, and releasing a crotonic acid and/or oligomers of crotonyl end group.¹⁹ The primary degradation products may undergo further decomposition above the melting temperature to form pyrolysis products. Similar to P3HB, P3HB3HV4HV copolymers may generate various degradation products including the monomeric crotonic acid, 2-pentanoic acid, as well as the oligomers with crotonyl or 2-pentanoyl end groups as shown in Scheme 1. Thus, it is very interesting to know whether or not the different monomers (3HB, 3HV, and 4HV) in PHA backbones have the same vulnerability in thermal degradation. If not, which monomer is more vulnerable? Many studies on PHA thermal degradation are conducted in a relatively narrow temperature range, either around

Additional Supporting Information may be found in the online version of this article.

© 2014 Wiley Periodicals, Inc.



Scheme 1. The structures of oligomers and monomers formed in thermal degradation of P3HB3HV4HV terpolyester.

melting point to study the thermal stability in melting, or at very high temperature to study thermal decomposition or pyrolysis. In the latter case, the products are often analyzed with GC/MS or nuclear magnetic resonance (NMR) without separation of the degradation products.^{9,11} Size exclusion chromatography plus NMR (SEC-NMR) analysis may reveal more information because it can separate the degradation products or oligomers according to their molecular size and then determine their unsaturated end groups. The relative abundance of the end groups derived from different monomers may reveal the vulnerability of the monomers in copolyesters.

In this work, we investigated the thermal stability and degradation of P3HB3HV4HV copolymers over a broad temperature range (100–300°C) in comparison with P3HB homopolyester. The thermal degradation kinetics of P3HB3HV4HV was investigated at constant temperatures below 190°C, and nonisothermal degradation was performed above 190–300°C. Two reaction models were applied for estimation of the activation energies in two temperature ranges. In addition, we also investigated a potential thermal processing technology by which the PHA bioplastics are processed at a temperature below the complete melting point. The vulnerability of 3HB and 3HV monomers in random P3HB3HV4HV copolymers was investigated at high temperatures (240–290°C).

EXPERIMENTAL

Materials

A natural blend of P(3HB-co-3HV-co-4HV) (P3HB3HV4HV) terpolyesters, named as Sample A thereafter, was synthesized from cosubstrates of glycerol and levulinic acid by a laboratory mutant strain of *Cupriavidus necator* in previous work.¹⁸ Sample A was further separated into four fractions (Samples A1, A2, A3, and A4 thereafter) by using solvent fractionation as described previously.¹⁸ A random P3HB3HV4HV copolymer (named as Sample D thereafter) was prepared from levulinic acid as the sole carbon source in a flask culture (see Table I). A

P3HB homopolymer (named as P3HB thereafter) was produced on glycerol as the sole carbon source in our previous work.²⁰ The PHA samples were purified by repeated dissolution, filtration and precipitation with chloroform and hexane. Polymer films of approximately 100- μm thickness were prepared by casting PHA-chloroform solutions onto Teflon Petri dishes and allowing the solvent to evaporate for 1 week to reach a constant weight. The solvent-casted films were further aged in vacuum at 50°C for at least 1 week and subsequently stored at room temperature for a month prior to use.

Thermal Degradation and Pyrolysis Test

Thermal degradation around the melting point (100–190°C) of PHA samples was investigated with a TA Instruments Q2000 Modulated differential scanning calorimetry (DSC) under a nitrogen flow of 50 mL min⁻¹. Polyester samples (~6 mg) were encapsulated in aluminum pans, heated from ambient to a predetermined temperature at 10°C min⁻¹, and isothermal degradation under nitrogen was conducted at the temperature for a predetermined time. The treated PHA samples were collected for further analysis.

Pyrolysis of P3HB3HV4HV was investigated with thermogravimetric analysis (TGA) by using a TA Instruments TGA Q500 under nitrogen as a purge gas. About 2 mg of each sample was heated from room temperature to 600°C at a heating rate of 20°C min⁻¹.

Isothermal pyrolysis was conducted for random PHA terpolyesters (Sample D). About 50 mg of PHA film sample was placed in a small glass reactor vial and sealed with a screw cap in air for 5 min. The vial was then put in a preheated oven (240 or 290°C) for 60 min. The treated products were analyzed with SEC, ¹H-NMR, and Fourier transform infrared spectroscopy (FTIR).

Analytical Procedures

The thermal properties of PHA samples (~3 mg film) were measured with a TA Instruments Q2000 DSC equipped with a

Table I. Composition and Properties of PHA Samples Used in This Study

| Sample | PHA composition (mol %) ^a | | | Thermal properties | | | | Molecular weight ^b | | <i>D</i> ^c |
|-------------------|---|------|-----|-----------------------------|-----------------------------|-----------------------------|-----------------------------------|-------------------------------|---|-----------------------|
| | 3HB | 3HV | 4HV | <i>T</i> _{m1} (°C) | <i>T</i> _{m2} (°C) | <i>T</i> _{m3} (°C) | ΔH_m (J g ⁻¹) | <i>M</i> _n (kDa) | <i>M</i> _w / <i>M</i> _n | |
| A ^d | 79 | 18.5 | 2.5 | 79 | 159 | 173 | 56 | 276 | 2.1 | 2.4 |
| A1 ^d | 96 | 3.5 | 0.5 | - | 162 | 176 | 83 | 320 | 2.5 | ND |
| A2 ^d | 81 | 15.8 | 3.2 | 75 | 116 | - | 59 | 530 | 1.6 | 1.5 |
| A3 ^d | 72 | 24.5 | 3.5 | 80 | 106 | - | 43 | 254 | 1.9 | 1.3 |
| A4 ^d | 62 | 34 | 4 | 74 | 100 | - | 32 | 129 | 2.1 | 1.1 |
| D ^e | 38 | 55 | 7 | 60 | - | - | 36 | 482 | 2.2 | 1.0 |
| P3HB ^f | 100 | 0 | 0 | - | 161 | 176 | 91 | 218 | 2.3 | ND |

ND, not determined; *T*_m, melting temperature; ΔH_m , enthalpy of fusion; *M*_n, number-average molecular weight; *M*_w, weight-average molecular weight; *M*_w/*M*_n, polydispersity.

^aPHA monomer composition of isolated PHA samples was determined by 500 MHz ¹H-NMR.

^bMolecular weight of PHA copolyesters.

^cRandomness parameter reported in the previous study.¹⁸

^dSample A is a natural blend of P3HB3HV4HV terpolyesters produced from fed-batch fermentation of glycerol and levulinic acid cosubstrates for 60 h. Sample A1, A2, A3, and A4 are random P3HB3HV4HV terpolymers fractionated from the Sample A with chloroform/*n*-hexane, as reported in the previous study.¹⁸

^eSample D is a random P3HB3HV4HV terpolyester produced from flask culture for 48 hours with multiple feedings of levulinic acid (10 g L⁻¹ = 4 × 2.5 g L⁻¹) as a sole substrate, as reported in the previous study.¹⁸

^fGlycerol-based P3HB.²⁰

refrigerated cooling system. Scanning was conducted under a nitrogen flow of 50 mL min⁻¹ from -50 to 200°C at a heating and cooling rate of 10°C min⁻¹. The melting temperature (*T*_m) and enthalpy of fusion (ΔH_m) were determined from the DSC thermograms.

SEC, Shimadzu LC-10AD HPLC system equipped with a RI detector (Shimadzu, Japan), and two Shodex mixed-bed K805L columns in series (Showa Denko, Tokyo, Japan) was used to measure the molecular weight and distribution of the original PHA samples and the products from thermal degradation and pyrolysis tests above. The samples dissolved in hot chloroform were eluted with chloroform at 1 mL min⁻¹. The molecular weights were calibrated with narrow-cut polystyrene standards (Sigma-Aldrich, St. Louis, MO), and the average molecular weights were calculated from the distribution curves using the manufacturer's SEC software (Shimadzu, Japan).

PHA samples were dissolved in CDCl₃ (25 mg mL⁻¹) via mild mixing and heating and analyzed with ¹H- and ¹³C-NMR spectroscopy (Varian Unity Inova 500 and 125 MHz) to find the monomer composition, chemical structure and polymer-sequence information. The thermal degradation products were also subjected to SEC separation as above and the fractions were collected in vials (3 mL) and the solvent chloroform was evaporated under room conditions. The dried products were then dissolved in deuterated chloroform (CDCl₃) for NMR analysis. The SEC-NMR analysis revealed the molecular weight and chemical structure of degradation products collected in separate fractions.

The infrared absorption spectra of PHA samples were recorded with a Nicolet Avatar 370 FTIR spectrometer (Thermo Electron Co., Madison, WI). All measurements were taken in air on a

diamond crystal window of microhorizontal attenuated total reflectance (ATR) with a GladiATR temperature controller. The PHA film sample was heated at a rate of 5°C min⁻¹ and the FTIR spectra were collected at room temperature to 200°C by signal averaging 32 scans at resolution of 4 cm⁻¹ in the wave number range of 4000–400 cm⁻¹. The film was exposed to 200°C (complete melting) and 140°C (partial melting), respectively, for a very short period time (<1 min) and cooled down quickly at a rate of 5°C min⁻¹. The nonisothermal crystallization process was monitored by recording FTIR spectra with time till 25°C. The partially crystallized PHA films were kept on ATP window for continuing crystallization and aging at 25°C and FTIR spectra were collected over 300 min till no further crystallization was observed. The fully crystallized films were kept in a desiccator for X-ray analysis. For thermally degraded products, the samples were pressed directly onto the ATR window and the absorption spectra were recorded. All data were processed with standard OMNIC software of the FTIR manufacturer.

Wide-angle X-ray diffraction (WAXD) patterns of PHA samples were recorded at 27°C on a Rigaku MiniFlexII system using nickel-filtered Cu K α radiation ($\lambda = 0.154$ nm; 30 kV; 15 mA) in the 2θ range 4–60° at a scan speed of 2.0° min⁻¹. The degree of crystallinity for PHA films was calculated from diffracted intensity data using Vonk's method.²¹

RESULTS AND DISCUSSION

Isothermal Degradation and Kinetic Analysis

Table I summarizes the chemical composition, melting temperature (*T*_m), molecular weight, and randomness of PHA samples used in this study. We investigated the thermal behavior and

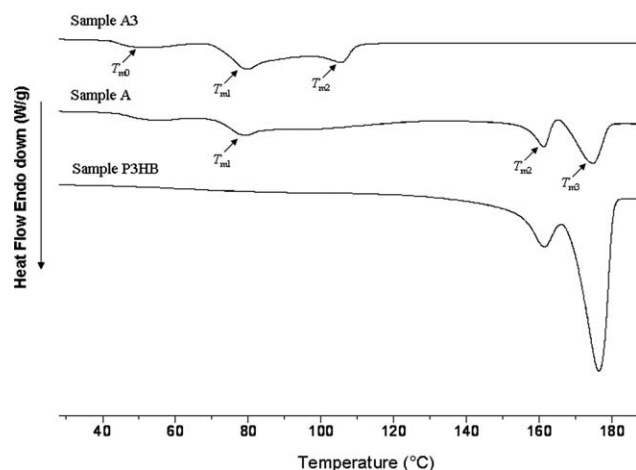


Figure 1. DSC first-scan thermograms of Samples P3HB, A, and A3 at a heating rate of $10^{\circ}\text{C min}^{-1}$.

degradation of P3HB, a natural blend of P3HB3HV4HV copolymers (Sample A), and one fraction of Sample A (Sample A3). Figure 1 exhibits the DSC thermograms of the samples during the first heating scan. Multiple endothermic peaks were observed for each sample. Three major peaks (T_{m1} , T_{m2} , and T_{m3}) were detected for Sample A, and a broad low temperature range (T_{m1} , $70\text{--}140^{\circ}\text{C}$) represents the melting characteristic of the Fraction A3, while the high melting peaks (T_{m2} , 159°C and T_{m3} , 173°C) reflect the typical melting behavior of P3HB.

Isothermal degradation studies were carried out with DSC under nitrogen atmosphere at temperature around respective T_m for 0, 2, 10, or 20 min. Table II lists the change in the number-

average molecular weight (M_n) and polydispersity during thermal degradation ($100\text{--}190^{\circ}\text{C}$). The samples had no measurable weight loss after 20 min thermal treatment. At temperature below 150°C , the M_n values of Sample A, an original P3HB3HV4HV copolymer containing 79% 3HB, 18.5% 3HV and 2.5% 4HV, did not decline very much with time. The M_n of Sample P3HB and A3 were almost unchanged over a period of 10 min at 150°C . This result indicates that the Fraction A3 can be completely melted in a temperature range of $70\text{--}120^{\circ}\text{C}$ without thermal decomposition. It may determine the melt stability of original P3HB3HV4HV in the broad low temperature range. In contrast, at temperatures above 170°C , the M_n values of all samples declined rapidly with time. For example, the M_n value of Sample A decreases to only 12% of the initial M_n after 20 min at 190°C , indicating a substantial degradation during a complete melt processing. All PHA samples exhibit a unimodal distribution of molecular weight and their polydispersity remained relatively narrow during the thermal degradation.

The thermal degradation of P3HB and other P3HB-based copolymers at temperature between 100 and 300°C is proposed to follow a random scission mechanism.^{22–24} If the scission rate is independent of the molecular weight and of the position of the scission in a given chain and no volatilization occurs during the thermal degradation, the inverse of the number-average degree of polymerization ($1/P_n$) is a linear function of the reaction time (t),

$$1/P_n - 1/P_0 = k_d t \quad (1)$$

where $1/P_0$ is the initial number average degree of polymerization and k_d is the rate constant of the reaction. The degradation

Table II. Change in Molecular Weight of PHA Samples and Their Degradation Kinetic Parameter During Thermal Degradation at Different Temperatures

| Sample | Degradation temperature ($^{\circ}\text{C}$) | $\times 10^3 M_n (M_w/M_n)^a$ | | | | $\times 10^{-5} k_d^b (\text{min}^{-1})$ |
|--------|--|-------------------------------|-----------|-----------|-----------|--|
| | | 0 min | 2 min | 10 min | 20 min | |
| P3HB | 150 | 198 (2.4) | 191 (2.4) | 189 (2.4) | | 0.16 |
| | 170 | 189 (2.3) | 154 (2.3) | 127 (2.4) | | 2.01 |
| | 180 | 186 (2.3) | 147 (2.2) | 80 (2.3) | | 6.13 |
| | 190 | 155 (2.4) | 106 (2.4) | 49 (1.9) | | 11.9 |
| A | 100 | 274 (2.3) | 270 (2.2) | 245 (2.2) | 223 (2.2) | 0.38 |
| | 110 | 261 (2.4) | 254 (2.1) | 213 (2.4) | 211 (2.4) | 0.43 |
| | 120 | 257 (2.3) | 250 (2.2) | 207 (2.4) | 191 (2.5) | 0.63 |
| | 130 | 248 (2.4) | 240 (2.2) | 210 (2.3) | 186 (2.6) | 0.61 |
| | 150 | 230 (2.4) | 214 (2.2) | 173 (2.5) | 148 (2.8) | 1.07 |
| | 170 | 213 (2.3) | 184 (2.3) | 98 (2.1) | 95 (2.1) | 5.04 |
| | 180 | 185 (2.4) | 134 (2.5) | 48 (2.3) | 38 (2.2) | 14.1 |
| | 190 | 145 (2.4) | 110 (2.4) | 35 (2.1) | 33 (1.8) | 20.0 |
| A3 | 100 | 248 (2.0) | 240 (1.9) | 236 (1.9) | | 0.19 |
| | 120 | 231 (2.1) | 214 (2.0) | 213 (1.9) | | 0.28 |
| | 150 | 221 (2.0) | 218 (1.9) | 212 (2.0) | | 0.20 |
| | 180 | 187 (2.0) | 167 (2.0) | 114 (1.9) | | 3.15 |

^a Molecular weight was determined by SEC.

^b Degradation rate constants of random chain scission.

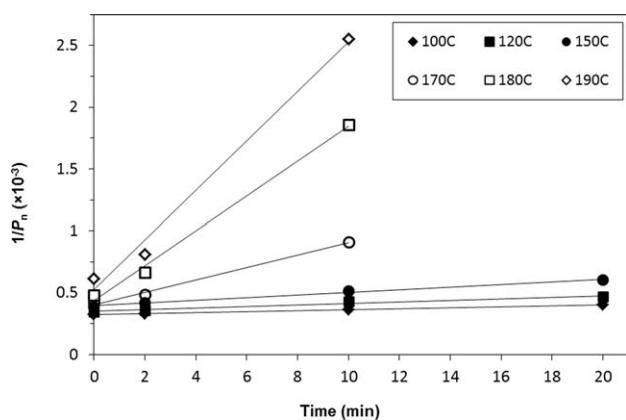


Figure 2. Changes in inverse of number-average degree of polymerization ($1/P_n$) during isothermal degradation of a natural PHA blend (Sample A) at various degradation temperatures.

rate constants (k_d) of three PHA samples were determined from the slopes of $1/P_n$ versus time [eq. (1)] and the values were listed in Table II. It can be observed that k_d values were less than 10^{-6} min^{-1} at temperature below 150°C .

Figure 2 shows the plots of $1/P_n$ with time for P3HB3HV4HV blend (Sample A) at different temperatures. At temperature below 150°C , a linear increase in $1/P_n$ with time was observed for 20 min, indicating that the thermal degradation followed a kinetic model of random scission. In contrast, at temperature above 170°C , the linear decrease in P_n occurs for a much shorter reaction time (10 min). After that, $1/P_n$ had a nonlinear relationship with time (not shown in Figure 2), which might be attributed to auto-acceleration by the low-molecular-weight products.¹¹ The effect of temperature on thermal degradation of P3HB and P3HB3HV4HV is determined by the activation energy (E_a) of individual reactions, which can be calculated by using the Arrhenius model [eq. (2)],

$$k_d = A e^{-E_a/RT} \quad (2)$$

where A is the frequency factor (h^{-1}), E_a is the activation energy (kJ mol^{-1}), T is the isothermal degradation tempera-

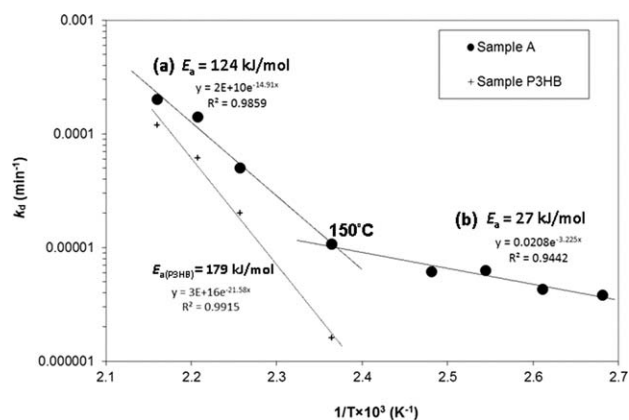


Figure 3. Linearized plots of Arrhenius model for thermal degradation of Samples A and P3HB in the ranges of (a) $150\text{--}190^\circ\text{C}$ and (b) $100\text{--}150^\circ\text{C}$.

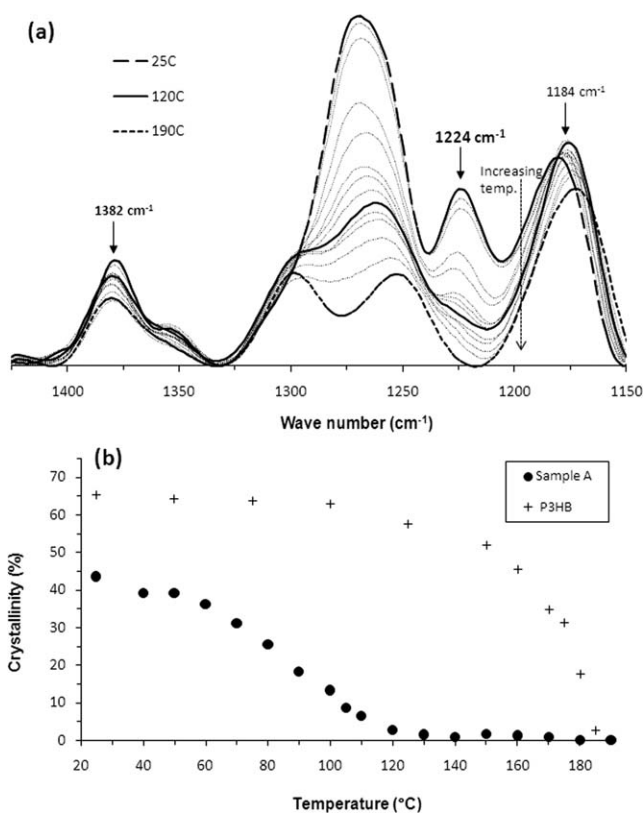


Figure 4. (a) *In situ* FTIR spectra of Sample A and (b) crystallinity plots of Samples P3HB and A during heating process from 25 to 190°C .

ture (K), and R is the gas constant ($8.3 \text{ J K}^{-1} \text{ mol}^{-1}$). The values of A and E_a are estimated from the plots of $\ln(k_d)$ against $1/T$ over a range from $100\text{--}190^\circ\text{C}$ and $150\text{--}190^\circ\text{C}$ for Sample A and P3HB, respectively, as shown in Figure 3. The activation energy (E_a) of random chain scission was estimated from the slopes of the Arrhenius plots.

It shows that the thermal degradation of P3HB3HV4HV (Sample A) actually falls in two temperature regions as reflected by two discontinuous straight lines of k_d versus $1/T$. The activation energy at temperature above 150°C [the left section (a) in Figure 3] is 124 kJ mol^{-1} , which is not very much lower than 179 and 182 kJ mol^{-1} of P3HB found in this study (dot line) and another study,¹⁶ respectively. In contrast, the apparent E_a value of P3HB3HV4HV (Sample A) at temperature below 150°C [the left section (b) in Figure 3] is only 27 kJ mol^{-1} , indicating a different degradation mechanism below 150°C . It has been widely accepted that the thermal degradation of P3HB or its related copolymers occurs through a six-member ring ester decomposition reaction.⁹ The discontinuity of P3HB3HV4HV degradation observed in this study may be attributed to a transition from the random scission model at high temperature that is not influenced by different monomers, to a random scission model at low temperature that is markedly affected by 3HV and 4HV. A practical question is whether or not at this transient temperature (around or below 150°C), thus the P3HB3HV4HV copolymer blend (Sample A) can be processed. This is addressed in the following section.

Elucidation of Melt Processability with *In Situ* ATR-FTIR

Thermal processing of P3HB3HV4HV at temperatures below 150°C has a technical merit, because the bioplastic exhibits a high thermal stability at or below this temperature. Below the temperature of complete melting (>150°C), however, the crystalline of the bioplastic may cause some problems in thermal processing. FTIR can provide qualitative and quantitative information on the structural changes in PHAs during melting and crystallization process.^{25,26} In this work, ATR-FTIR was used to monitor the *in situ* material transition from a semicrystalline solid to an amorphous melt when P3HB3HV4HV copolymer was heated to the temperatures near 150°C, and its crystallization.

Figure 4(a) shows the temperature dependence of the infrared absorption spectra of Sample A in the wavenumber range of 1150 to 1450 cm⁻¹ collected *in situ* during the heating process from ambient temperature (25°C) to melting temperature (190°C). The absorbance at a crystalline band (1224 cm⁻¹) decreases steadily with temperature increase. In previous studies,^{25–28} the degree of crystallinity of P3HB was monitored with FTIR at two representative wavenumbers 1184 and 1224 cm⁻¹, corresponding to the asymmetric stretching of C—O—C backbone in the amorphous phase, and the asymmetric stretching of C—C—C bond in the crystalline phase, respectively. The absorbance at wavenumber 1382 cm⁻¹ corresponds to the symmetric bending of the CH₃ group in P3HB and is taken as a reference peak because its intensity is insensitive to the change in crystallinity of PHA.²⁷

By using WAXD that can directly measure the crystallinity of a semicrystalline polymer, we compared the IR absorption intensities at three wave numbers and the X-ray crystallinity of fully crystallized P3HB3HV4HV films (Samples A and A1–A4) and an amorphous P3HB as shown in Figure 5(a). The absorbance at 1224 cm⁻¹ changes closely with the WAXD crystallinity, while the amorphous band at 1184 cm⁻¹ was not sensitive to the change in crystallinity. A crystallinity index (CI_{*i*}) is defined as the absorbance ratio of the crystalline band at 1224 cm⁻¹ to the reference band at 1382 cm⁻¹ [eq. (3)].

$$CI_i = A_{1224} / A_{1382} \quad (3)$$

where A_{1224} is the absorption intensity at 1224 cm⁻¹ and A_{1382} is the absorption intensity at 1382 cm⁻¹. The real crystallinity from FTIR spectrograms, the values of CI_{*i*} are correlated with those values measured by WAXD as shown in Figure 5(b). The calibration curve between the real crystallinity (%) and the IR index is also shown in Figure 5(b) that give rise on a slope value about 64.2%. Therefore, calculated percentage of crystallinity could be assigned with eq. (4).

$$\text{Crystallinity}(\%) = 64.2 \times (A_{1224} / A_{1382}) \quad (4)$$

where A_{1224} and A_{1382} are the absorbance intensities at 1224 and 1382 cm⁻¹, respectively. Figure 4(b) shows the *in situ* crystallinity of P3HB3HV4HV (Sample A) and P3HB during melting process from 25–190°C. When Sample A was heated from 25 to 140°C, the crystallinity declined gradually from 44 to 0%. In another word, the P3HB3HV4HV is in amorphous phase with no crystallinity (0%) at 140°C or above. This fact indicates

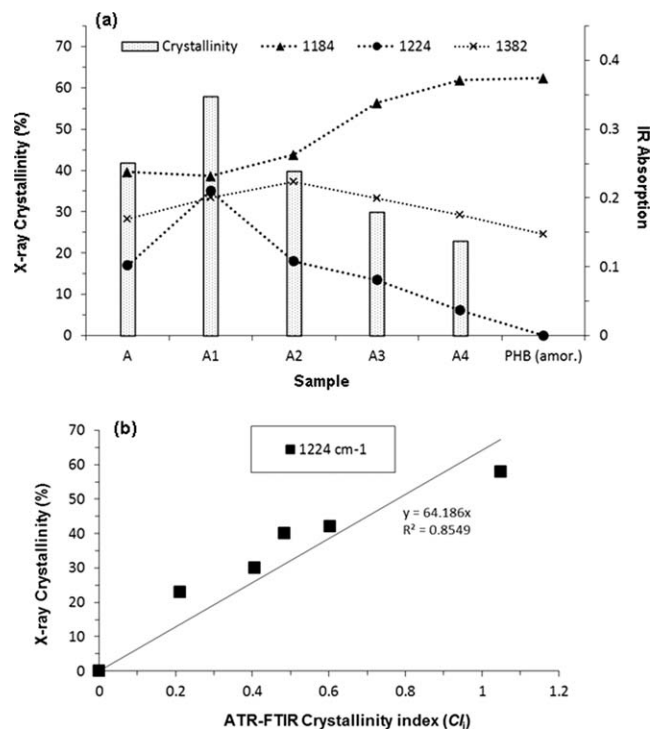


Figure 5. (a) Infrared absorption measured at wavenumbers 1180, 1224, and 1380 cm⁻¹ and degree of X-ray crystallinity of crystalline films of the series of Sample A and melted P3HB (amorphous state); (b) relation between the crystallization index calculated from FTIR and the absolute crystallinity determined from WAXD.

that Sample A was gradually melted starting at 70°C and ended at 140°C, in agreement with the broad melting range of DSC endotherm in Figure 1. At 140°C, the P3HB3HV4HV sample was in a state of semisolid and semiliquid, but in complete amorphous phase. More interestingly, its molecular weight declined very slowly because of good thermal stability at the low temperature. As reported in our previous work,¹⁸ Sample A is a miscible blend of P3HB3HV4HV copolymers consisting of Fractions A1 to A4. As shown in Table I, Fraction A1 (33 wt % of original P3HB3HV4HV mass) has a high content of 3HB and a relatively high melting temperature, while Fractions A2, A3, and A4 account for 67 wt % and exhibit a low melting range because of high content of 3HV and 4HV. Thus, the overall thermal behavior of Sample A is markedly affected by the Fractions of high 3HV and 4HV content. The Fraction A1 of high 3HB content may act as a nucleation agent in crystallization of the blend (Sample A). For comparison, the crystallinity of P3HB declined more abruptly at 150°C and dropped to zero from 185°C as shown in Figure 4(b). The melting of P3HB reached the maximum rate around 180°C, in agreement with the sharp peak of DSC curve at 176°C.

To simulate the low-temperature processing at 140°C, the melt P3HB3HV4HV (Sample A) was cooled down to room temperature and *in situ* crystallization process was monitored on ATR-FTIR. Figure 6(a) shows the temperature and aging development of infrared absorption spectra illustrating the nonisothermal crystallization of the Sample A cooled from a semisolid

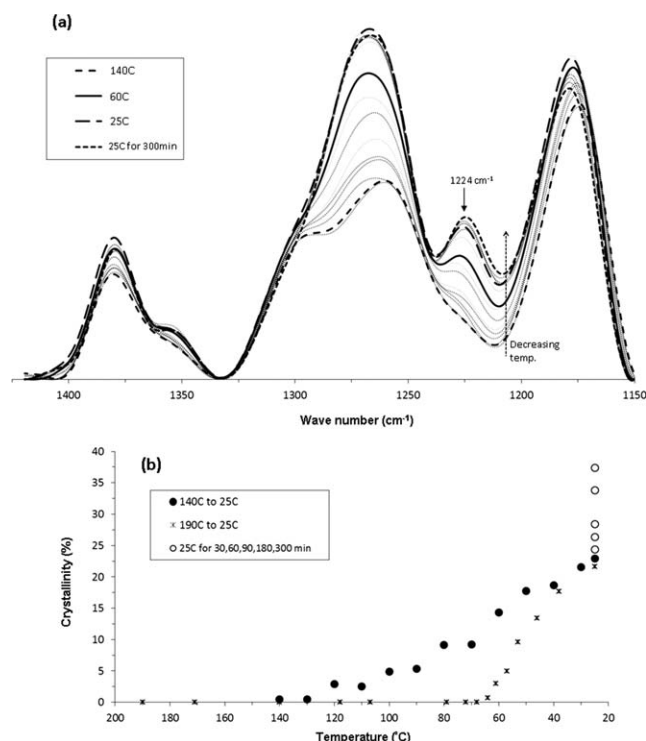


Figure 6. (a) *In situ* FTIR spectra and (b) crystallinity plot of the P3HB3HV4HV copolymer blend (Sample A) during cooling process of nonisothermal crystallization from 140 and 190°C to ambient temperature (25°C).

amorphous state at 140°C to a semicrystalline solid at 25°C, followed by aging for 300 min in ambient conditions. The absorption intensities of the crystalline band at 1224 cm⁻¹ increased gradually during the cooling and aging process, while the absorbance at 1382 cm⁻¹ had little change. The crystallization processes of Sample A melted at 140 and 190°C, respectively, are shown in Figure 6(b). Starting at 140°C, crystallization was observed at about 120°C, and the crystallinity gradually increased to 24% at 25°C. After 300 min aging, the crystallinity further increased to and maintained at 39%. In contrast, starting at 190°C, the initial crystallization was observed at 65°C, and the crystallinity abruptly increased to 22%. The delayed crystallization may be attributed to the reduced molecular weight because of thermal degradation at 190°C. P3HB3HV4HV should therefore be melted and molded around 140°C because of (a) fast crystallization and solidification, (b) high thermal stability, and (c) good mechanical properties of plastic goods.

Nonisothermal Degradation with TGA

TGA is a popular tool to study nonisothermal decomposition of polymers.^{19,29} Figure 7(a,b) is the thermogravimetric (TG) curves, and differential thermogravimetric (DTG) curves of P3HB homopolymer (Sample P3HB) and a random P3HB3HV4HV terpolymer containing 38% 3HB, 55% 3HV, and 7% 4HV (Sample D in Table I) at a heating rate of 20°C min⁻¹ under nitrogen gas. The TG curves reflect gradual weight loss of the samples and the DTG curves indicate the rate increase in weight loss (dw/dt) with temperature, which peaked at 306 and 300°C for Sample P3HB and D, respectively.

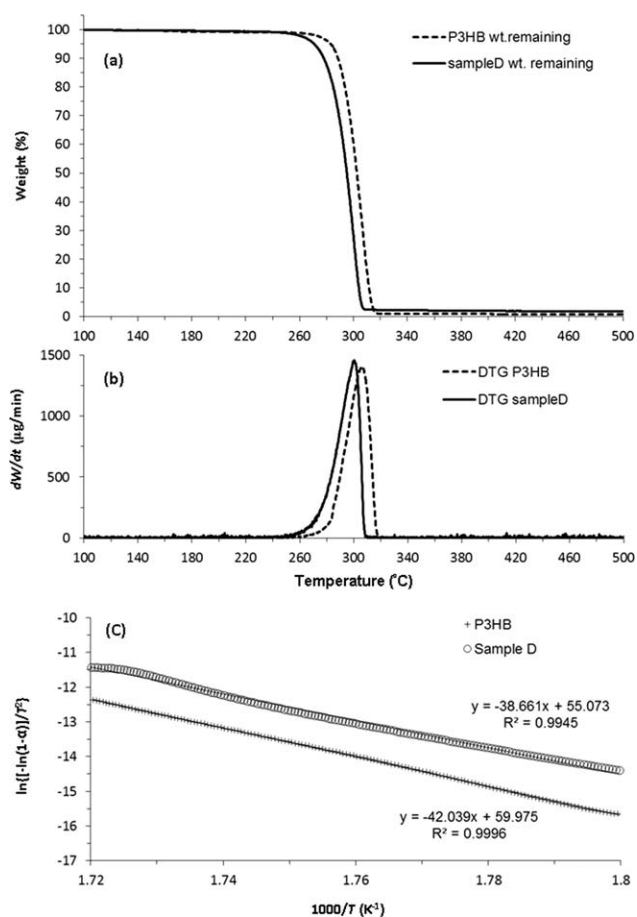


Figure 7. (a) TG and (b) DTG curves of Samples P3HB and D at a heating rate of 20°C min⁻¹ under nitrogen condition. (c) Plots of $\ln[-\ln(1-\alpha)]/T^2$ vs. $1000/T$ in the ranges of 282–308°C for TG data in first-order reaction ($n=1$) as following through the Coats–Redfern integral method.

Table III lists the onset decomposition temperature which is determined by the temperature of 5 wt % weight loss ($T_{d,-5\%}$), the midpoint temperature of thermal decomposition ($T_{d,-50\%}$), the solid residue, and the temperature of the maximum weight loss rate ($T_{d,max}$). For Sample D, the 5% weight loss starts at around 271°C, and the carbonaceous residue is almost zero (~1.8%) at 309°C. The decompositions of random P3HB3HV4HV (Sample D) and P3HB had almost the same pattern with slightly reduced thermal stability of P3HB3HV4HV. This fact implies that under severe thermal degradation conditions, the monomers of 3HV and 4HV do not significantly affect the stability of polyester backbone dominated by 3HB.

To obtain additional information on the mechanism of thermal degradation and/or decomposition, the activation energy is estimated with a kinetic model [eq. (5)]. The reaction kinetic parameters are estimated by fitting the TG data with the Coats–Redfern integral method.³⁰

$$d\alpha/dt = k_d(1-\alpha)^n \quad (5)$$

With the Arrhenius equation [eq. (2)], the following equations [eqs. (6) and (7)] are obtained:

Table III. TGA Data and Kinetic Parameters of Random P3HB3HV4HV (Sample D) and P3HB in Nonisothermal Degradation

| Sample | Temperature at specific weight loss (°C) | | | Residue ^a (%) | E_a^b (kJ mol ⁻¹) |
|-----------------------|--|-----------------|---------------|--------------------------|---------------------------------|
| | $T_{d,-5\%}^c$ | $T_{d,-50\%}^d$ | $T_{d,max}^e$ | | |
| P3HB | 283 | 303 | 306 | 0.8 ± 0.2 | 349 |
| P3HB3HV4HV (Sample D) | 271 | 295 | 300 | 1.8 ± 0.3 | 321 |

^a The solid residue from TG curve.^b Activation energy calculated from Coats-Redfern integral method.³⁰^c The temperature of 5 wt % weight loss.^d The temperature of 50 wt % weight loss.^e The temperature of the maximum weight loss rate from DTG curve.

$$\ln \left\{ \frac{[1 - (1 - \alpha)^{1-n}]/[T^2(1-n)]}{(1 - 2RT/E_a)AR/BE_a} - E_a/RT \right\} \quad (6)$$

when $n = 1$:

$$\ln [-\ln(1 - \alpha)/T^2] = \ln [(1 - 2RT/E_a)AR/BE_a] - E_a/RT \quad (7)$$

where n is the reaction order, α is the reaction degree representing the fractional extent of conversion (i.e., weight loss), T is the absolute temperature, R is the gas constant, B is the heating rate, and A is the frequency factor. In this study, we assume a first reaction order ($n = 1$), as it gives highly correlated coefficients as shown in Figure 7(c). The plots of $\ln[-\ln(1 - \alpha)/T^2]$ versus $1/T$ have a good linearity ($R^2 > 0.99$), and the value of $-E_a/R$ is estimated from the slope. The apparent activation energy of thermal decomposition of a random P3HB3HV4HV (Sample D; $E_a = 321$ kJ mol⁻¹) was slightly lower than that of Sample P3HB ($E_a = 349$ kJ mol⁻¹) (Table III). It seems that the thermal decomposition of random P3HB3HV4HV terpolymer

(Sample D) follows the same mechanism of P3HB, which is not affected to a great extent in the presence of 3HV and 4HV monomers.

Thermal Degradation Products of P3HB3HV4HV Under Air

¹H-NMR analysis is a useful method for identification and characterization of thermal degradation products under severe conditions. Specifically, we combined this method with SEC in which the residues were separated into fractions according to their molecular sizes and then the chemical structures of products in each fraction were identified with ¹H-NMR. A random P3HB3HV4HV terpolymer (Sample D) with high 3HV content was heated under air to and then maintained at 240 or 290°C for 60 min, respectively, referring to the $T_{d,-50\%}$ observed in the TG curve [Figure 7(a)]. At these temperatures, the polymer was degraded into interesting products in liquid and gas phases. The liquid products were dissolved in chloroform and separated into 5 to 7 fractions with SEC. Table IV lists the fractions and their

Table IV. SEC Fractions and ¹H-NMR Analysis of Degradation Products of P3HB3HV4HV (Sample D) at 240°C or 290°C Under Air

| Sample | Fraction no. (f) | Temp. (°C) | Residual PHA oligomer (monomer content, mol %) | | | End-group ratio | | M_w (kDa) | SEC area (%) |
|--------|------------------|------------|--|------|-----|--------------------|--|-------------|--------------|
| | | | 3HB | 3HV | 4HV | HV/HB ^a | CH ₃ /CH ₂ of 3HV ^b | | |
| D | | 240 | 41.2 | 52.0 | 6.8 | 1.0 | 1.6 | 2.6 | 100 |
| | 1 | | 37.1 | 56.0 | 6.9 | - | - | 80 | 7.4 |
| | 2 | | 38.0 | 54.1 | 7.8 | - | - | 10 | 14.9 |
| | 3 | | 50.1 | 44.6 | 5.3 | 0.4 | 1.5 | 5.0 | 28.9 |
| | 4 | | 51.9 | 44.4 | 3.7 | 0.5 | 1.4 | 1.7 | 23.2 |
| | 5 | | 63.1 | 35.8 | 1.1 | 1.9 | 1.9 | 0.7 | 6.3 |
| | 6 | | 75.9 | 23.4 | 0.7 | 1.1 | 1.5 | 0.09 | 9.6 |
| | 7 | | ND | ND | ND | 1.5 | 0.5 | 0.03 | 9.7 |
| D | | 290 | 53.9 | 41.1 | 5.0 | 1.4 | 1.5 | 0.6 | 100 |
| | 1 | | 37.3 | 59.3 | 3.4 | - | - | 9.0 | 3.2 |
| | 2 | | 38.6 | 57.9 | 3.5 | 0.3 | 0.3 | 2.3 | 4.5 |
| | 3 | | 41.0 | 52.0 | 7.0 | 0.7 | 1.7 | 0.9 | 10.4 |
| | 4 | | 60.7 | 34.4 | 4.9 | 1.1 | 1.6 | 0.6 | 3.9 |
| | 5 | | 71.0 | 27.4 | 1.6 | 4.0 | 1.5 | 0.09 | 78.0 |

ND, not detected.

^a Ratio of methyl proton (CH₃) resonances of crotonyl and 2-pentanoyl chain ends (assignment ratio of 7 : 3).^b Ratio of methyl proton (CH₃) and methylene (CH₂) resonances of 2-pentanoyl chain end (assignment ratio of 7 : 6).

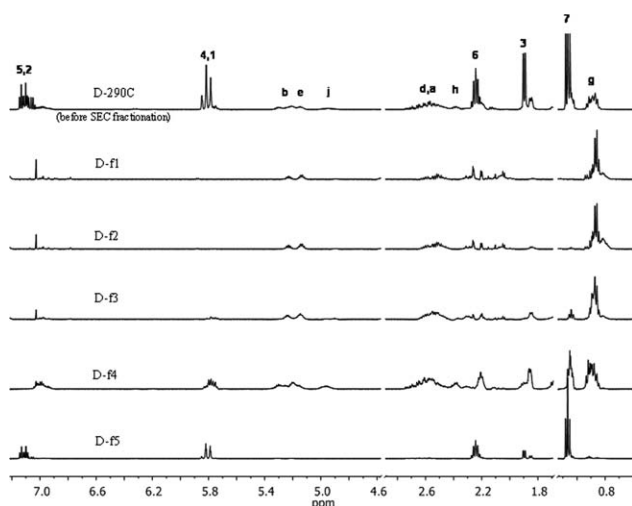


Figure 8. $^1\text{H-NMR}$ spectra of random P3HB3HV4HV copolymer (Sample D) and of its SEC fractions. The proton resonances were assigned corresponding to the chemical structure in Scheme 1.

results of $^1\text{H-NMR}$ analysis. Figure 8 shows the $^1\text{H-NMR}$ spectra of degradation product of P3HB3HV4HV (Sample D) and its five SEC fractions with peak assignments according to Scheme 1. The spectra clearly indicate that the residual oligomers contained a carboxylic acid end group (3HB, 3HV, and 4HV) and an unsaturated end group (crotonyl and 2-pentanoyl chain ends, or crotonic acid, and 2-pentanoic acid), as expected from the previous discussion on *cis*-elimination reaction.

The NMR resonances of a–h are assigned to the methyl (CH_3), methylene (CH_2), and methane (CH) proton resonances of 3HB, 3HV, and 4HV oligomers as seen in Scheme 1 and our previous report.¹⁸ The strong resonances of 3, 6, and 7 are assignable to the proton resonances of methyl of crotonyl chain end, methylene, and methyl of 2-pentanoyl chain end, respectively. The additional peaks of 4,1 and 5,2 are attributed to olefinic protons in the crotonyl or 2-pentanoyl end groups, resulting from the P3HB3HV4HV random chain scission. As seen in Figure 8, the fractions of Sample D have a significant variation in the chemical structure of oligomers. The details in chemical composition and end-group ratio can be found in Table IV. The SEC-NMR analysis in Table IV reveals a significant change in the monomer composition and molecular weights of the residual oligomers at two temperatures. The fractions with low molecular weights exhibited a low 3HV content and a high 3HB content. For example, in the products of Sample D treated at 290°C, 3HV content of oligomers declined from 59.3 to 27.4, as the molecular mass decreases from 9000 Da (Fraction 1) to 90 Da (Fraction 5) with SEC area of 3.2 and 78%, respectively. In Table IV, we also see that the intensity ratio of HV methyl proton (Signal 7) to HB methyl proton (Signal 3) gradually increases with decrease in molecular weight fraction, indicating formation of more 2-pentanoyl chain ends (from 3HV transesterification) than crotonyl chain ends (from 3HB transesterification). No product with end group derived from 4HV was found in the NMR spectra, most likely because of the very low content (< 8%) of 4HV in the terpolyesters. The chain end analysis therefore does not include 4HV-derived

products. To confirm the correction of the chain-end analyses, the intensity ratio of HV methyl proton (Signal 7) to HV methylene proton (Signal 6) was also calculated, and the values of all the samples are close to 1.5, similar to the proton ratio of methyl and methylene (3 : 2). These results indicate that 3HV unit is more vulnerable to thermal degradation than 3HB unit because more 3HV ends were formed in the smaller oligomers. This was also confirmed with matrix-assisted laser desorption-ionization time-of-flight mass spectrometry (MALDI-TOF-MS) by measuring the M-Na^+ adducts of different hydroxyalkanoate repetitive units in the products of the pyrolyzed sample D thermally degraded at 290°C without separation as shown in Figure S1 of the Supporting Information section. It was clear that the analysis found more 3HV species (100-Na^+ m/z) than 3HB species (86-Na^+ m/z) in smaller oligomers.

This interesting phenomenon is first time found in this study, because to authors' knowledge there is no report with clear experimental evidence on the thermal vulnerability of different monomers in PHA copolyesters. Possibility has been suggested in the literature that the 3HV unit may have an adverse effect on the overall thermal stability of poly(3HB-*co*-3HV) copolymers.^{11,13,31} This study provides an experimental evidence to confirm that the second monomer such as 3HV does have some adverse effect on the overall thermal stability of copolyesters particularly under severe conditions. This may be explained by using the degradation mechanism. The 3HV monomer unit has a longer side chain than 3HB does, and it is easier for 3HV to form a transient structure of a six-member ring during thermal degradation via *cis*-elimination reaction.^{9,32} The transient ring structure is shifted towards formation of 2-pentanoyl chain end oligomers and 2-pentanoic acid, resulting in a fraction of high HV chain-end group and low molecular weight, such as Fraction D-f5 at 290°C.

CONCLUSIONS

- Two different activation energies of P3HB3HV4HV copolymers were found in the range of 100–190°C. The two lines of thermal degradation kinetics cross at 150°C. Below 150°C, the biopolyester exhibited a high thermal stability.
- Although the semicrystalline P3HB3HV4HV is melted completely above 180°C, it became an amorphous semisolid around 140°C. The natural blend of P3HB3HV4HV can therefore be processed at a low temperature with excellent thermal stability.
- At high temperatures (190–300°C), pyrolysis of P3HB3HV4HV under nitrogen occurs. The apparent activation energy of nonisothermal thermal degradation of P3HB3HV4HV was slightly lower than that of P3HB indicating a similar degradation mechanism.
- By using a new method of SEC-NMR analysis, it is found that the 3HV unit in P3HB3HV4HV copolymers is more vulnerable to thermal degradation than the 3HB unit when the biopolyester is heated to high temperatures under air.

ACKNOWLEDGMENTS

The authors appreciate the NMR analysis performed by Wesley Yoshida of the Chemistry Department, University of Hawaii at

Manoa. Additionally, we thank Office of Research, Academic Affairs and Innovations, Faculty of Medicine Ramathibodi Hospital, Mahidol University for MALDI-TOF-MS experiments.

REFERENCES

1. Anderson, A. J.; Dawes, E. A. *Microb. Mol. Biol. Rev.* **1990**, *54*, 450.
2. Lenz, R. W.; Marchessault, R. H. *Biomacromolecules* **2004**, *6*, 1.
3. Luzier, W. D. *Proc. Natl. Acad. Sci.* **1992**, *89*, 839.
4. Witholt, B.; Kessler, B. *Curr. Opin. Biotechnol.* **1999**, *10*, 279.
5. Sudesh, K.; Abe, H.; Doi, Y. *Prog. Polym. Sci.* **2000**, *25*, 1503.
6. Chen, G.-Q. *Chem. Soc. Rev.* **2009**, *38*, 2434.
7. Chanprateep, S. J. *Biosci. Bioeng.* **2010**, *110*, 621.
8. Lehrle, R. S.; Williams, R. J. *Macromolecules* **1994**, *27*, 3782.
9. Kunioka, M.; Doi, Y. *Macromolecules* **1990**, *23*, 1933.
10. Ariffin, H.; Nishida, H.; Shirai, Y.; Hassan, M. A. *Polym. Degrad. Stab.* **2008**, *93*, 1433.
11. Nguyen, S.; Yu, G.-E.; Marchessault, R. H. *Biomacromolecules* **2001**, *3*, 219.
12. Lee, M. Y.; Lee, T. S.; Park, W. H. *Macromol. Chem. Phys.* **2001**, *202*, 1257.
13. Morikawa, H.; Marchessault, R. H. *Can. J. Chem.* **1981**, *59*, 2306.
14. Aoyagi, Y.; Yamashita, K.; Doi, Y. *Polym. Degrad. Stab.* **2002**, *76*, 53.
15. Kopinke, F. D.; Mackenzie, K. J. *J. Anal. Appl. Pyrol.* **1997**, *40-41*, 43.
16. Kim, K. J.; Doi, Y.; Abe, H. *Polym. Degrad. Stab.* **2006**, *91*, 769.
17. Kim, K. J.; Doi, Y.; Abe, H. *Polym. Degrad. Stab.* **2008**, *93*, 776.
18. Tanadchangsang, N.; Yu, J. *J. Appl. Polym. Sci.* **2013**, *129*, 2004.
19. Abe, H. *Macromol. Biosci.* **2006**, *6*, 469.
20. Tanadchangsang, N.; Yu, J. *Biotechnol. Bioeng.* **2012**, *109*, 2808.
21. Vonk, C. G. *J. Appl. Crystallogr.* **1973**, *6*, 148.
22. Grassie, N.; Murray, E. J.; Holmes, P. A. *Polym. Degrad. Stab.* **1984**, *6*, 47.
23. Grassie, N.; Murray, E. J.; Holmes, P. A. *Polym. Degrad. Stab.* **1984**, *6*, 127.
24. Grassie, N.; Murray, E. J.; Holmes, P. A. *Polym. Degrad. Stab.* **1984**, *6*, 95.
25. Xu, J.; Guo, B. H.; Yang, R.; Wu, Q.; Chen, G. Q.; Zhang, Z. M. *Polymer* **2002**, *43*, 6893.
26. Porter, M.; Yu, J. *Microbiol. Methods.* **2011**, *87*, 49.
27. Bloembergen, S.; Holden, D. A.; Hamer, G. K.; Bluhm, T. L.; Marchessault, R. H. *Macromolecules* **1986**, *19*, 2865.
28. Sato, H.; Murakami, R.; Padermshoke, A.; Hirose, F.; Senda, K.; Noda, I.; Ozaki, Y. *Macromolecules* **2004**, *37*, 7203.
29. Li, S.-D.; He, J.-D.; Yu, P. H.; Cheung, M. K. *J. Appl. Polym. Sci.* **2003**, *89*, 1530.
30. Coats, A. W.; Redfern, J. P. *Nature* **1964**, *201*, 68.
31. Mitomo, H.; Ota, E. *Sen'I Gakkaishi* **1991**, *47*, 89.
32. Yu, J.; Plackett, D.; Chen, L. X. L. *Polym. Degrad. Stab.* **2005**, *89*, 289.